Comparison of AZO, GZO, and AGZO Thin Films TCOs Applied for a-Si Solar Cells

Y. C. Lin, T. Y. Chen, L. C. Wang and S. Y. Lien

J. Electrochem. Soc. 2012, Volume 159, Issue 6, Pages H599-H604.
doi: 10.1149/2.108206jes

Journal of The Electrochemical Society, **159** (6) H599-H604 (2012)
0013-4651/2012/159(6)/H599/6/$28.00 © The Electrochemical Society

Comparison of AZO, GZO, and AGZO Thin Films TCOs Applied for a-Si Solar Cells

Y. C. Lin,[a,z] T. Y. Chen,[a] L. C. Wang,[a] and S. Y. Lien[b]

[a]*Department of Mechatronics Engineering, National Changhua University of Education, Changhua 50007, Taiwan*
[b]*Department of Materials Science and Engineering, MingDao University, ChungHua 52345, Taiwan*

This study prepared aluminum and gallium co-doped zinc oxide (AGZO) thin films using pulsed direct current magnetron sputtering, and studied the electrical properties, transmittance, effects of texturing, and applicability as the front contact for a-Si:H solar cells. Textured ZnO:Al (AZO) and ZnO:Ga (GZO) thin films were also compared with AGZO thin film to evaluate their performance as front contacts. Experimental results show that AGZO films with the highest figure of merit ϕ_{TC} value ($24.64 \times 10^{-3}\ \Omega^{-1}$) were obtained at Al and Ga doping concentrations of 0.54 wt% and 1.165 wt%, respectively. The textured AGZO films used as the front contact in a-Si:H solar cells achieved the following results: $V_{OC} = 0.77$ V, $J_{SC} = 16.5$ mA/cm^2, FF = 59%, and conversion efficiency of 7.53%. AZO and GZO films have better electrical properties than AGZO film; however, AGZO film has superior transmittance in the near-infrared (NIR) region and higher J_{SC}, conversion efficiency and external quantum efficiency (EQE) than AZO and GZO films under a similar haze value.
 [DOI: 10.1149/2.108206jes]

Manuscript submitted October 28, 2011; revised manuscript received April 10, 2012. Published April 20, 2012.

In recent years, transparent conducting oxide (TCO) thin films have been applied in silicon thin film solar cells, providing high transparency in the visible light region and good electrical conductivity.[1–3] Light scattering in silicon thin film solar cells can be achieved using wet-etching, to produce surface structures capable of scattering incident light into the silicon absorber layer.[4–6]

For amorphous silicon solar cells, SnO_2:F (Asahi U-Type) and AZO have been the most favored TCOs.[7] GZO has better conductivity and transparency in the near infrared region.[8–10] Meanwhile, AZO has relatively low thermal stability and problems with degeneration following extended exposure to ambient air, due to the high reactivity of Al.[11–13]

Previously, Kang et al.[14] co-sputtered AZO and GZO to prepare AGZO film and studied the electrical and optical properties. Lee et al.[8] studied the damp heat stability of AGZO film before and after annealing. The present study is the first to evaluate the performance of AGZO as a front contact in a-Si:H solar cell. Three common TCOs (ZnO-based AZO, GZO, AGZO thin films) were applied and differences in the performance of each solar cell were investigated. AGZO was deposited using pulsed DC magnetron sputtering and a light trapping structure was formed by wet-etching.

Experimental

This study employed pulsed direct current magnetron sputtering to deposit the AGZO thin films on the glass substrate measuring 25×25 mm^2. To study the influence of Al doping concentration (0.42–0.74 wt%) on the characteristics of the thin films, the position of the metallic Al sheet on the GZO target material was varied to alter the doping concentration of Al within the GZO. A sintered ceramic GZO target (3 inch in diameter with thickness 6 mm) was doped with 0.6 wt% Ga_2O_3. The purity of the Al sheet (1 mm in height and 2 mm in diameter) was 99.99%. The pulsed magnetron sputtering process was performed at a working pressure of 0.4 Pa, power of 150 W, substrate temperature of 373 K, and thickness of 800 nm. AGZO films were post-annealed at 473–873 K for 30 minutes in an argon atmosphere. Prior to application to the front contact of a-Si:H solar cells, AGZO films were textured for various durations using 0.5% and 0.3% diluted HCl so as to form light trapping structures. An energy dispersive spectrometer (Hitachi S3000N) was used to analyze the chemical composition, and an X-ray photoelectron spectroscope (XPS, PHI 5000, VersaProbe) with Al Kα (1486.6 eV, width 0.85 eV) was used to analyze the chemical state of the films. Hall effect measurements (ECOPIA HMS-2000) were used to determine resistivity, mobility, and carrier concentration. X-ray diffraction (XRD, SHIMADZU XRD-6000) with Cu Kα radiation was used to analyze the crystal structure.

Haacke's new figure of merit was adopted to determine the quality of the AGZO films. Haacke[15] defined a new figure of merit for transparent conductor oxide films, as shown in the Eq. 1:

$$\phi_{TC} = T^{10}/R_s \quad [1]$$

where T is the average transmission at 550 nm, and R_s is the sheet resistance of the transparent conductor oxide films. Additionally, the energy gap (E_g) of AGZO film was determined by the Tauc relationship[16,17] as following:

$$\alpha h\nu = k(h\nu - E_g)^{1/2} \quad [2]$$

where α is the optical absorption coefficient, $h\nu$ is the photon energy, and k is the proportional constant. An extrapolating of the linear plot of $(\alpha h\nu)^2$ on the y-axis versus photon energy ($h\nu$) on the x-axis produces a value of E_g at $(\alpha h\nu)^2 = 0$. The surface features and surface roughness of AGZO films were observed using a thermal field emission scanning electron microscope (JEOL TF-SEM JSM7000F). A fiber coupled CCD array spectrometer (Hon Ming MFS-630) was used to measure the haze value in the wavelength range of 250–900 nm.

To compare the electrical properties, transmittance, and photovoltaic performance with common ZnO-based TCOs (i.e. AZO and GZO), the GZO target (3 wt% Ga_2O_3) and AZO target (2 wt% Al_2O_3) were adopted for the deposition of GZO[12] and AZO films[18] using pulsed magnetron sputtering at a substrate temperature of 473 K, followed by texturing for application to the front contact of a-Si:H solar cells. In addition, to investigate the surface roughness of films after textured, this study used atomic force microscopy (AFM, Solver NT-MDT P47) measurement.

Finally, p-i-n a-Si:H thin film solar cells were deposited by PECVD under a working pressure of 90 Pa, at a substrate temperature of 473 K, and power of 10 W to deposit a p-layer 8 nm-thick, buffer layer 6 nm-thick, intrinsic-layer 300 nm-thick and n-layer 20 nm-thick on textured AGZO, AZO, and GZO films on a glass substrate. Ag back contacts were prepared by sputtering. Details of the cell structure can be found in Ref. 19. Following fabrication, the solar cells were annealed at 150°C for 2 h. By adopting a textured surface for the front contact (AGZO, AZO, and GZO) the optical path of the light is increased through scattering, thereby increasing absorption in the active layers. The current-voltage and EQE characteristics of the solar cellswere measured at 100 mW/cm^2 using an AM 1.5 solar simulator. The effective aperture area of the cell is 20×20 mm^2 by laser scribing process.

[z]E-mail: ielinyc@cc.ncue.edu.tw

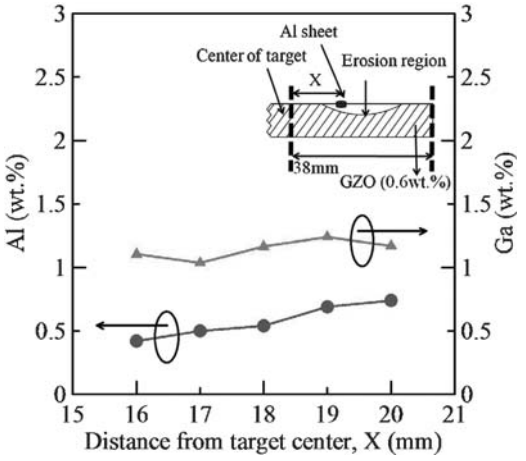

Figure 1. Correspondence chart of metallic Al location and Ga content on GZO target, produced at a power of 150 W, working pressure of 0.4 Pa, substrate temperature of 373 K, and film thickness of 800 nm.

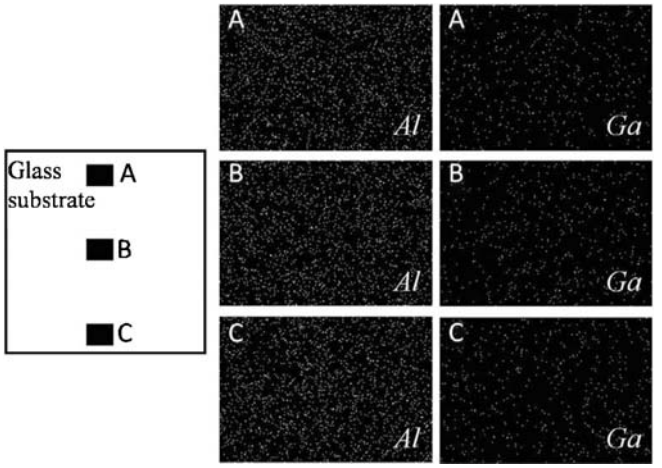

Figure 3. The stoichiometry mapping image of Al and Ga elements in various locations of AGZO film with Al doping concentration 0.54 wt%.

Results and Discussion

Characteristics and surface texturing of AGZO.— The position of the Al sheet was changed to alter the Al doping concentration. EDS analysis of the AGZO films showing the relative position X of the Al sheet and GZO target can be seen in Fig. 1. An increase in the distance from target center, X of Al sheet and GZO target increased the doping concentration of Al. We computed ϕ_{TC} values according to Eq. 1, for various doping concentrations, as shown in Fig. 2. In addition, the stoichiometry mapping image of Al and Ga elements in various locations of sample can be seen in Fig. 3. The EDX measured result shows that the distribution of Al and Ga elements are uniform from different locations of sample. When AGZO films were prepared and then annealed under argon atmosphere at 473–873 K for 30 minutes at a doping concentration of 0.54 wt%, the highest ϕ_{TC} values were 24.64 $\times 10^{-3}$ Ω^{-1}, as shown in Fig. 4. The highest ϕ_{TC} value of 28 $\times 10^{-3}$ Ω^{-1} was obtained at an annealing temperature of 473 K and ϕ_{TC} values decreased with an increase in annealing temperature. At an annealing temperature of 473 K, the electrical and optical properties of AGZO films exceeded those of as-deposited AGZO. Variations in the energy gap of AGZO with an Al doping concentration of 0.54 wt% following annealing are shown in Fig. 5. The highest energy gap of 3.63 eV was observed at an Al doping concentration of 0.54 wt%, which did not increase with an increase in carrier concentration, implying that excessively high Al doping concentrations would lead to ion scattering and a decrease in mobility, influencing absorption in the blue light

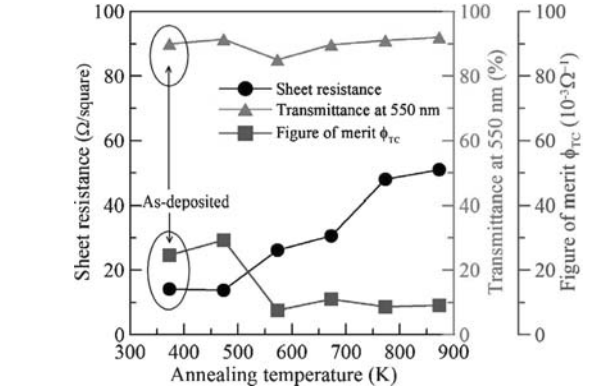

Figure 4. Figure of merit for AGZO films with Al doping concentration 0.54 wt%, under various annealing temperatures. AGZO films were prepared at a power of 150 W, working pressure of 0.4 Pa, substrate temperature of 373 K, and film thickness of 800 nm.

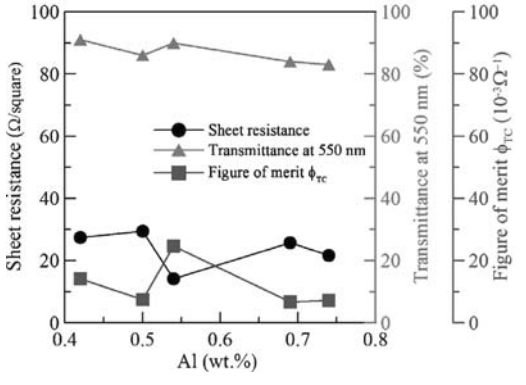

Figure 2. Figure of merit of AGZO films with various Al doping concentrations, produced at a power of 150 W, working pressure of 0.4 Pa, substrate temperature of 373 K, and film thickness of 800 nm.

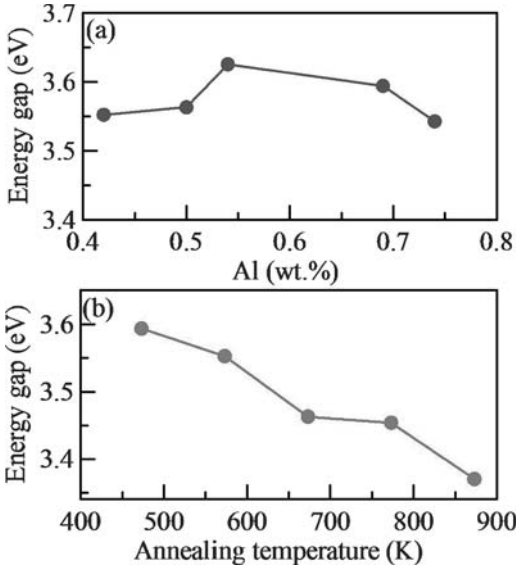

Figure 5. Variations in energy gap of AGZO films: (a) with different Al doping concentration; (b) annealed at 473 K–873 K.

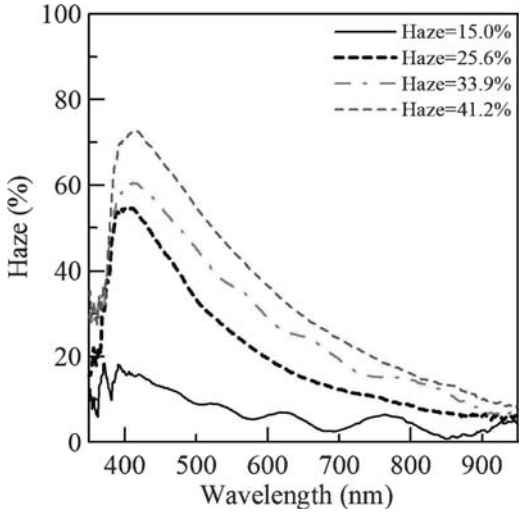

Figure 6. Haze spectrum of textured AGZO films with Al doping concentration of 0.54 wt%, under various texturing condition at room temperature to obtain an average haze value at 380–800 nm. (haze = 15.0%: 0.3% HCl for 14s; haze = 25.6%: 0.3% HCl for 22s; haze = 33.9%: 0.5% HCl for 3s, haze = 41.2%: 0.5% HCl for 7s).

region as well as a decrease in the energy gap.[20] After annealing, the energy gap decreased with an increase in annealing temperature, which could be attributed to a decrease in carrier concentration. This would lead to a reduction in carrier concentration and a decrease in energy gap due to the Burstein-Moss effect.[21]

AGZO films with an Al doping concentration of 0.54 wt% were textured using 0.5% and 0.3% diluted HCl to form a light trapping structure. Fig. 6 shows the haze spectrum of AGZO films under various texturing conditions at room temperature. AGZO texturing using 0.5% diluted HCl resulted in a higher haze value, despite the reduction in etching time. The influence of damage to the surface of the films was more obvious following etching at higher concentrations of diluted HCl. An increase in etching time resulted in a more pronounced textured effect on the surface of the films, thereby improving the light trapping structure and increasing the optical path of incident light. A higher haze value implies higher diffuse transmittance at the surface of the film.

SEM images of the surface structure of textured AGZO films are shown in Fig. 7. When the AGZO films were textured using 0.3% diluted HCl solution, particle clusters were formed on the surface of the film; however, light trapping structures are not obvious. With an increase in etching time, the number of particle clusters increased, with a subsequent increase in the roughness of film resulting in enhanced diffusion of incident light. When the AGZO films were textured using 0.5% diluted HCl solution, craters were observed on the surface of the film and an increase in etching time increased the roughness of the film as well as the diameter of the craters (220–780) nm. A higher degree of roughness results in better light trapping effect, indicating good light diffusion potential. It is worth to mention, the particle clusters formed on the surface of the film is only appear when the AGZO films were textured using 0.3% diluted HCl solution for a longer etching time. The EDS spectrum measured shown that the composition of particle mainly includes aluminum and oxygen elements. The diminished etch behavior using 0.3% diluted HCl solution may prefer to etch Ga than Al, and resulting in an Al_2O_3 particle formed on the surface of the film. But, Al_2O_3 particle will be etched under a stronger 0.5% diluted HCl solution.

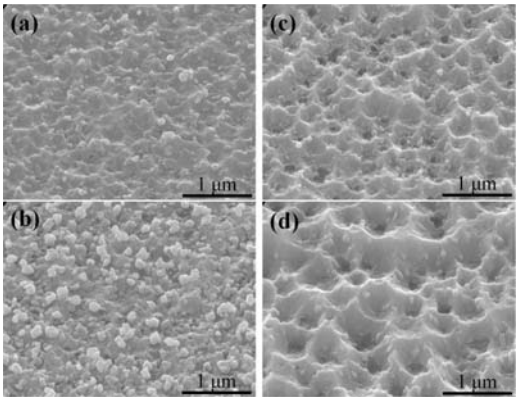

Figure 7. Surface features of textured AGZO films with Al doping concentration 0.54 wt% under various texturing conditions at the room temperature. The SEM images were taken at an oblique angle of 10°–15°: (a) 0.3% HCl for 14s; (b) 0.3% HCl for 22s; (c) 0.5% HCl for 3s; and (d) 0.5% HCl for 7s.

Table I. Hall effect measurements of AGZO, AZO, and GZO films.

Sample	Resistivity (Ωcm)	Mobility ($cm^2V^{-1}S^{-1}$)	Carrier concentration (cm^{-3})
AGZO	8.14×10^{-4}	13.5	6.35×10^{20}
AZO	4.31×10^{-4}	22.0	11.09×10^{20}
GZO	3.18×10^{-4}	27.8	11.05×10^{20}

Comparison of AGZO, AZO, and GZO.— A comparison of AGZO, AZO, and GZO films reveals that AZO and GZO films have better electrical properties (lower resistivity and higher mobility and carrier concentration) than AGZO film, due to their higher doping concentrations and lager grain size (see XRD analysis in Fig. 9). Hall measurements are shown in Table I, and transmittance in the wavelength range of 300–2000 nm is shown in Fig. 8. In the visible light range, the average transmittance remained above 80%. In the shorter wavelength range of 350–380 nm, the optical band edge of AZO and GZO shifted to the blue light region. In the range of 800–2000 nm, the average transmittance of AGZO (59.5%) exceeded that of AZO (41.8%) and GZO (30.4%). The sheet resistance and surface roughness measurements at various conditions in AZO, GZO, and AGZO film is showed in Table II.

Liu et al.[13] described how the transmittance spectra at 300–2000 nm shifted to the blue region with an increase in doping carrier concentration, due to the Burstein-Moss effect. The average transmittance

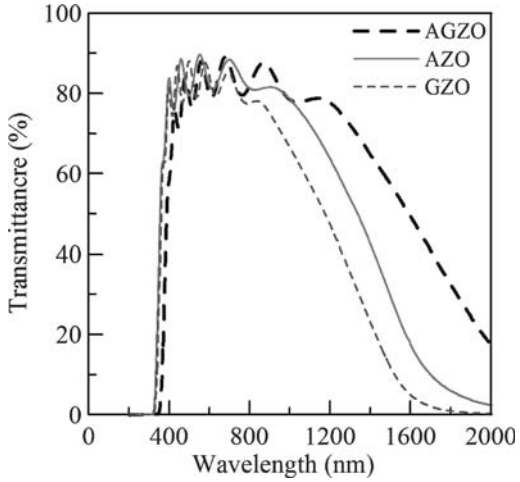

Figure 8. Transmittance in the wavelength range of 300–2000 nm for AZO,GZO, and AGZO films.

Table II. Sheet resistance and surface roughness measurements of various conditions in AZO, GZO, and AGZO films.

	AZO		GZO		AGZO	
Condition	Sheet resistance (W/square)	Surface roughness (Rms, nm)	Sheet resistance (W/square)	Surface roughness (Rms, nm)	Sheet resistance (W/square)	Surface roughness (Rms, nm)
As-deposited	10.1	2.6	8.0	2.8	14.8	2.8
Annealed	5.9	2.7	4.4	2.8	11.2	2.8
After etching[a]	12.9	28.4	9.2	29.3	16.3	36.0

[a] Haze value : AZO = 22.7 %; GZO = 23.6 %; AGZO = 25.6 %

in the range of 800–2000 nm increased and the total transmittance spectra shifted to the blue light region. In addition, TCO is regarded as a plasma.[22] The carrier concentration of TCO is approximately 10^{19}–10^{21} cm^{-3}, and the corresponding plasma frequency and plasma wavelength are located in the NIR region, implying that free carriers have a considerable influence in the NIR region. According to the Drude-Lorentz model, plasma frequency increases with an increase in concentration; therefore, an increase in the attenuation coefficient in the NIR region would result in a decrease in the transmittance in the NIR region. Jin et al.[23] studied the reflectance and transmittance of AZO films of various concentrations. With an increase in Al doping concentration, transmittance in the NIR region decreased and the total transmittance spectra shifted to the blue light region.

XRD analysis for various thin films is shown in Fig. 9. All of the films exhibit a typical hexagonal wurtzite structure with a ZnO (002) preferential orientation. According to XRD, the peaks of GZO films (34.22°) are lower than those of AZO films (34.4°). The ionic radius of Ga (0.62 Å) is larger than that of Al (0.53 Å),[24] leading to a higher lattice constant and downward shift in diffraction peaks.[25] AGZO films contain Ga^{3+} ions and Al^{3+}, implying that the average ion radius is approximately 0.62–0.53 Å, and the peak (34.34°) is located between the peaks observed in AZO and GZO. The diffraction peak intensity and full width at half maximum (FWHM) of AGZO films are wider than those of AZO and GZO. According to Table I, AGZO has the highest resistivity, implying that the AGZO acquires more lattice defects during the deposition process.

In the XPS survey spectra shown in Fig. 10, an Al2p peak is observed in AZO films with possible binding energy in the oxidation state. A Ga3d peak was observed in GZO films with possible binding energy in the oxidation or metallic states. Peaks for Al2p and Ga3d were observed in AGZO films and the possible binding formula of Al2p is the oxidation state, while the possible binding formula of Ga3d is the oxidation or metallic state, Ga atom. As discussed previously, the binding formula of doped atoms, Al and Ga, in AGZO films did not change as they do in AZO and GZO films; however, the binding energy of the Al2p and Ga3d peaks in AGZO films increased slightly.

Performance of amorphous silicon thin films solar cells with AGZO.— I-V parameters of a-Si:H solar cells for AGZO films under various etching conditions are shown in Table III. The haze value was obtained according to the average value in the visible region (Fig. 6). Non-textured AGZO films had the highest V_{oc} of 0.84 V, because the texturing process led to the formation of cracks and current leakage at the AGZO/p-layer interface, resulting in a decrease in $V_{OC.}$[26] J_{SC} increased with an increase in haze value, with the highest J_{SC} of 16.53 mA/cm^2 obtained at a haze value of 33.92%. Due to the influence of light trapping structures, incident light was diffused at the AGZO/p-layer interface with a subsequent increase in the optical path enhancing optical absorption within the silicon layer. J_{SC} was improved from 13.21 mA/cm^2 to 16.53 mA/cm^2, and the conversion efficiency was also improved. When the haze value increased to 41.24%, J_{SC} decreased to 14.98 mA/cm^2. The thickness of the active layer of AGZO film after texturing to produce a haze value of 41.24% prevented the complete absorption of incident light. Textured AGZO

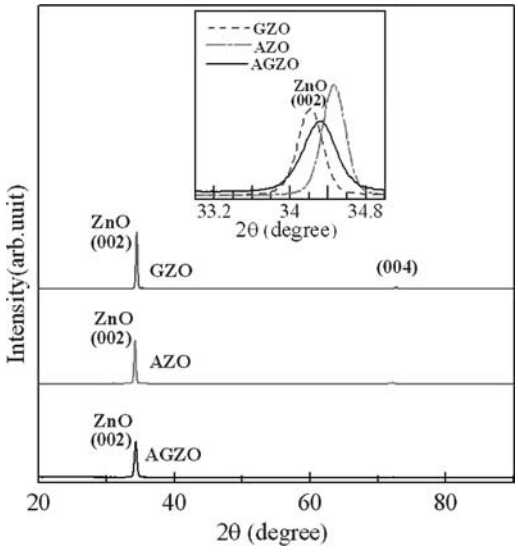

Figure 9. X-ray diffraction patterns for AZO, GZO, AGZO films. Lattice parameters are as follows: GZO: F /WHM = 0.0096 (lattice constant) = 1.3529Å, peak degree = 34.22°; AZO: FWHM = 0.0163, a: = .3378Å, peak degree = 34.4°; AGZO: FWHM = 0.0225, a = 1.34161Å, peak degree = 34.34°.

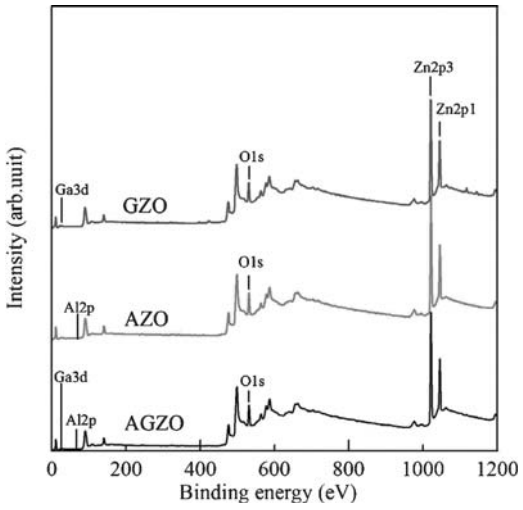

Figure 10. XPS survey spectra for AZO, GZO, AGZO films. Peak formula and binding energy of doped atoms for GZO films are 20.392 eV, Ga_2O_3, Ga; peak formula and binding energy of doped atom for AZO films are 74.86 eV, Al_2O_3; binding energy of doped atom for AGZO films are 20.392 eV and peak formulae are Ga_2O_3, Ga, Al_2O_3.

Table III. Performance of amorphous silicon thin films solar cells for AGZO films with various etching conditions.

Sample (haze%)	Voc(V)	Jsc(mA/cm^2)	FF%	η%
Non-textured	0.84	13.21	52.54	5.80
haze=15.0%	0.77	13.85	60.43	6.51
haze=25.6%	0.72	16.00	64.01	7.34
haze=33.9%	0.77	16.53	59.04	7.53
haze=41.2%	0.78	14.98	60.09	7.03

films with a haze value of 33.9% achieved the following results: FF = 59%, V_{OC} = 0.77 V, J_{SC} = 16.5 mA/cm^2, and efficiency of 7.53%.

Comparison of performance between AZO, GZO, and AGZO amorphous silicon thin films solar cells.— After texturing AZO, GZO, and AGZO were applied to amorphous silicon thin films solar cells. The haze curve of AZO, GZO, and AGZO films textured with textured with 0.3% diluted HCl for 40 s, 30 s and 22 s respectively is shown in Fig. 11. AZO had a haze value of 22.7% and GZO had a haze value of 23.6%. I-V characterization of a-Si:H solar cells with various front contacts is shown in Table IV. The V_{OC} was approximately 0.8–0.72 V. The J_{SC} of AZO and GZO were 12.9 mA/cm^2 and 13.3 mA/cm^2, respectively, which are lower than that of AGZO, implying that the photon collection ability of AGZO films exceeds that of the other two front contacts. The V_{OC} for GZO films was the highest, which can be attributed to superior conductivity. The AGZO coated sample has the highest FF of 0.64 could be attributed to a decrease in carrier concentration, with subsequent decrease in the number of Al^{3+} or Ga^{3+} ions diffusing into the p-layer, thereby alleviating the problem of pollution at the front contact/p-layer interface. (An increase in carrier concentration increases the probability of pollution at the front contact/p-layer interface resulting in poor cell performance[27]). Rech et al.[28] deposited AZO as a front contact in μc-Si:H solar cells using RF sputtering with different Al contents and obtained similar results.

The EQE of a-Si:H solar cells with various front contacts is shown in Fig. 12. In the range of 300–400 nm, the spectral response of AZO and GZO was higher than that of AGZO, due to the larger energy gap of AZO and GZO. In the range of 400–800 nm, the spectral response of AZO and GZO was lower than that of AGZO, implying that a higher optical utilization rate was responsible for the higher J_{SC}. AZO and GZO demonstrated lower J_{SC}, conversion efficiency, and EQE than AGZO. It seems to originate from different reflectance caused

Table IV. Performance of amorphous silicon thin films solar cells for AZO, GZO, and AGZO films.

Sample (haze%)	Voc(V)	Jsc(mA/cm^2)	FF%	η %
AGZO (25.6 %)	0.72	16.0	64.01	7.34
AZO (22.7 %)	0.72	13.1	58.2	5.48
GZO(23.6 %)	0.78	13.9	59.2	6.45

by different light scattering properties. Otherwise, Interface region seems that pollution atoms are possibly diffused into the silicon layer during the plasma process, affecting the carry recombination rate in the contact/p-layer interface and therefore the performance of solar cells.

Conclusions

In this study, AGZO thin films were prepared using pulsed direct current magnetron sputtering with various Al doping concentrations followed by annealing at 473–873 K and surface texturing with 0.5% and 0.3% diluted HCl. Finally, an a-Si:H layer and AZO/Ag contact were deposited to complete the solar cells. Experimental results reveal that AGZO films have the highest figure of merit ϕ_{TC} value (24.64 $\times$ 10^{-3} Ω^{-1}) at an Al doping concentration of 0.54 wt%. When produced at an annealing temperature of 473 K, the ϕ_{TC} value exceeded that of as-deposited AGZO films. AGZO films with a textured surface increase the optical path of light by means of scattering, thereby increasing absorption in the active layer resulting in improved EQE and conversion efficiency. Textured AGZO film with a haze value of 33.9% achieved the following results: FF = 59%, V_{OC} = 0.77 V, J_{SC} = 16.5 mA/cm^2, and conversion efficiency of 7.53%. AZO and GZO have better electrical properties, transmittance, and lattice characteristic than AGZO films; however, the transmittance in the NIR region decreases with an increase in carrier concentration due to the Drude-Lorentz model and the Burstein-Moss effect. As a front contact, AGZO has higher short circuit current density and external quantum efficiency than AZO and GZO. This could be attributed to a decrease in carrier concentration, with subsequent decrease in the content of Al^{3+} or Ga^{3+} ions diffusing into the p-layer, thereby alleviating the problem of pollution by dopants at the interface between front contact and p-layer. In addition, in the range of 800–1200 nm, AGZO has superior transmittance to that of AZO and GZO. AGZO films are suitable for application on tandem amorphous silicon solar cells as

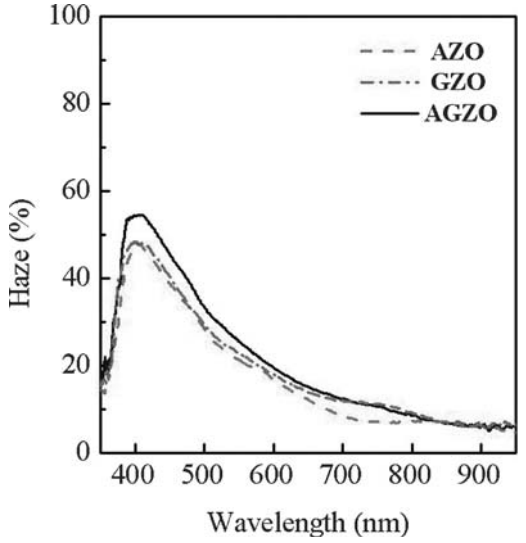

Figure 11. The haze curve of AZO, GZO, and AGZO films textured with 0.3% diluted HCl for 40 s, 30 s and 22 s respectively.

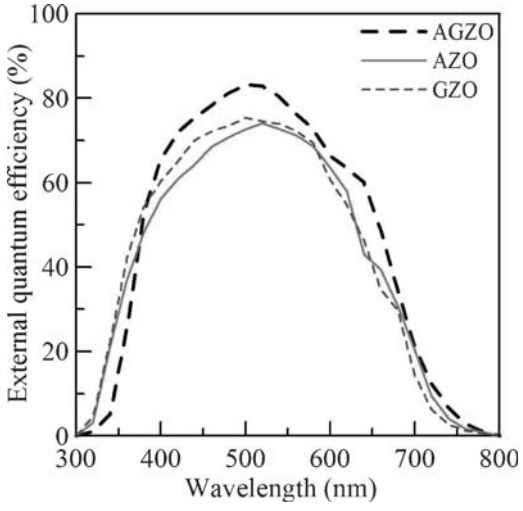

Figure 12. Quantum efficiency of amorphous silicon thin film solar cells for various front contacts. (AGZO: haze = 25.6%; AZO: haze = 22.7%; GZO: haze = 23.6%).

well as in CIGS solar cells, an application which is currently being studied.

References

1. J. Wienke, B. van der Zanden, M. Tijssen, and M. Zeman, *Sol. Energy Mater. Sol. Cells*, **92**, 884 (2008).
2. J. A. A. Selvan, A. E. Delahoy, S. Guo, and Y. M. Li, *Sol. Energy Mater. Sol. Cells*, **90**, 3371 (2006).
3. K. Lai, F. Tsai, J. Wang, C. Yeh, and M. Houng, *Sol. Energy Mater. Sol. Cells*, **95**, 1583 (2011).
4. R. Groenen, J. Löffler, P. M. Sommeling, J. L. Linden, E. A. G. Hamers, R. E. I. Schropp, and M. C. M. van de Sanden, *Thin Solid Films*, **392**, 226 (2001).
5. K. C. Lai, J. H. Wang, C. H. Lu, F. J. Tsai, C. H. Yeh, and M. P. Houng, *Sol. Energy Mater. Sol. Cells*, **95**, 415 (2011).
6. A. Krasnov, *Sol. Energy Mater. Sol. Cells*, **94**, 1648 (2010).
7. J. K. Rath, Y. Liu, M. Jong, J. Wild, J. A. Schuttauf, M. Brinza, and R. Schropp, *Thin Solid Films*, **518**, 129 (2010).
8. J. H. Kang, M. H. Lee, D. W. Kim, Y. S. Lim, W. S. Seo, and H. J. Choi, *Curr. Appl. Phys.*, S333 (2011).
9. S. H. Park, J. B. Park, and P. K. Song, *Curr. Appl. Phys.*, **10**, S488 (2010).
10. H. K. Park, J. W. Kang, S. I. Na, D. Y. Kim, and H. K. Kim, *Sol. Energy Mater. Sol. Cells*, **93**, 1994 (2009).
11. J. Hupkes, B. Rech, S. Calnan, O. Kluth, U. Zastrow, H. Siekmann, and M. Wuttig, *Thin Solid Films*, **502**, 286 (2006).
12. W. T. Yen, Y. C. Lin, P. C. Yao, J. H. Ke, and Y. L. Chen, *Thin Solid Films*, **518**, 3882 (2010).
13. H. Liu, V. Avrutin, N. Izyumskaya, U. Ozgur, and H. Morkoç, *Superlattices Microst.*, **48**, 458 (2010).
14. J. Kang, H. W. Kim, and C. Lee, *J. Korean Phys. Soc.*, **56**, 576 (2010).
15. G. Haacke, *J. Appl. Phys.*, **47**, 4086 (1976).
16. J. Tauc, *Amorphous and Liquid Semiconductors*, Plenum, New York, (1974).
17. A. F. Maged, A. M. Sanad, M. F. El-Fouly, and G. A. M. Amin, *J. Mater. Res.*, **13**, 1128 (1998).
18. W. T. Yen, Y. C. Lin, and J. H. Ke, *Appl. Surf. Sci.*, **257**, 960 (2010).
19. S. Y. Lien, C. C. Wang, C. T. Shen, Y. C. Ou, Y. S. Cho, K. W. Weng, C. H. Chao, C. F. Chen, and D. S. Wuu, *Thin Solid Films*, **518**, 7233 (2010).
20. Y. C. Lin, B. L. Wang, W. T. Yen, and C. H. Shen, *Thin Solid Films*, **519**, 5571 (2011).
21. I. Hamberg, C. G. Granqvist, K. F. Berggren, B. E. Sernelius, and L. Engström, *Phys. Rev.*, **30**, 3240 (1984).
22. T. J. Coutts, D. L. Young, and X. Li, *MRS Bull.*, **25**, 58 (2000).
23. Z. C. Jin, L. Hamberg, and C. G. Granqvist, *J. Appl. Phys.*, **64**, 5117 (1988).
24. F. Wu, L. Fang, Y. J. Pan, K. Zhou, Q. L. Huang, and C. Y. Kong, *Physica E*, **43**, 228 (2010).
25. H. Kato, M. Sano, K. Miyamoto, and T. Yao, *J. Cryst. Growth*, **237–239**, 538 (2002).
26. M. Python, O. Madani, D. Domine, F. Meillaud, E. V. Sauvain, and C. Ballif, *Sol. Energy Mater. Sol. Cells*, **93**, 1714 (2009).
27. H. Stiebig, F. Siebke, W. Beyer, C. Beneking, B. Rech, and H. Wagner, *Sol. Energy Mater. Sol. Cells*, **48**, 351 (1997).
28. B. Rech, T. Repmann, M. N. van den Donker, M. Berginski, T. Kilper, J. Hu¨pkes, S. Calnan, H. Stiebig, and S. Wieder, *Thin Solid Films*, **511–512**, 548 (2006).